Solid-State ^{13}C NMR Analyses of the Crystalline−Noncrystalline Structure for Metallocene-Catalyzed Linear Low-Density Polyethylene

Kazuhiro Kuwabara, Hironori Kaji, and Fumitaka Horii*

Institute for Chemical Research, Kyoto University, Uji, Kyoto 611, Japan

David C. Bassett and Robert H. Olley

J. J. Thomson Physical Laboratory, University of Reading, Whiteknights, Reading RG6 2AF, U.K.

Received April 28, 1997; Revised Manuscript Received August 7, 1997[⊗]

ABSTRACT: Solid-state ^{13}C NMR analyses have been performed to obtain information about the crystalline−noncrystalline structure for metallocene-catalyzed linear low-density polyethylene (MLLDPE) isothermally crystallized from the melt. ^{13}C spin−lattice relaxation time (T_{1C}) and ^{13}C spin−spin relaxation time (T_{2C}) analyses have revealed that three components with different T_{1C} and T_{2C} values exist for MLLDPE, which are assignable to the crystalline, crystalline−amorphous interfacial, and rubbery amorphous components. Using such differences in T_{2C}, we have separately recorded the spectra of interfacial and amorphous components and then resolved the fully relaxed DD/MAS spectrum of MLLDPE into the three components. As a result, it has been found that the thickness of the interfacial region is about 3 nm, in good accord with the previous result for bulk-crystallized high-density polyethylene (HDPE). $T_{1\rho H}$ and T_{2C} analyses have also revealed that butyl branches are excluded out from the crystalline region and are almost equally distributed in the crystalline−amorphous interfacial and amorphous regions. It has been also found that the molecular mobility is somewhat more enhanced in the interfacial region for MLLDPE compared with the case for HDPE. The same analysis is applied to Ziegler−Natta-catalyzed LLDPE isothermally crystallized from the melt as well as those quenched samples, and the crystalline−noncrystalline structures of the samples are discussed.

Introduction

Linear low-density polyethylene prepared by using metallocenes as catalyst has features of random distribution of branches and narrow distribution in molecular weight.[1−5] Although the solid structure based on such molecular characteristics may be closely associated with the excellent transparency and high impact strength of this polymer, the detailed solid structure is not revealed yet at present.

High-resolution solid-state ^{13}C NMR spectroscopy is very powerful in characterizing the detailed structure and molecular motions for different solid polymers.[6] In particular, we have clarified the phase structure composed of the crystalline, crystalline−amorphous interfacial, and amorphous regions for different crystalline polymers[7−13] by analyzing ^{13}C spin−lattice relaxation and spin−spin relaxation behaviors, ^{13}C resonance line shapes, and so on. The characteristic crystalline−noncrystalline structure has also been revealed for cellulose,[14−16] poly(vinyl alcohol),[17−19] and polyurethane elastomer[20] by similar ^{13}C NMR analysis.

In this work, we have characterized the crystalline−noncrystalline structure for metallocene-catalyzed and Ziegler−Natta-catalyzed linear low-density polyethylene samples by the similar solid-state ^{13}C NMR analysis previously employed, transmission electron microscopy (TEM), and differential scanning calorimetry (DSC).

Experimental Section

Samples. Linear low-density polyethylene (LLDPE) samples, synthesized with 1-hexene as a comonomer by metallocene catalysis or Ziegler−Natta catalysis, were used for bulk crystallization; These materials with butyl branches were pilot-plant resins obtained from Neste Oy Chemicals, their characteristics being listed in Table 1.[1] For each LLDPE, two types of crystallizing conditions were employed. The metallocene-catalyzed sample was isothermally crystallized at 110 °C for 18 h (MLLDPE) or quenched in liquid nitrogen from the melt and subjected to aging for about 7 days at room temperature (MQLLDPE). The material prepared by the Ziegler−Natta catalyst was isothermally crystallized at 110 °C for 2 h (ZLLDPE) or quenched in the same manner as that for MQLLDPE (ZQLLDPE). It should be noted here that the 18 h crystallization for MLLDPE gives almost the same morphology as the 2 h crystallization.[3]

Table 1. Characteristics of Nascent LLDPE Samples[a]

	LLDPE prepared from given methods	
	metallocene catalysis	Ziegler−Natta catalysis
comonomer content (wt %)		
solution-state ^{13}C NMR	5.4	5.6
IR		5.4
branch content (per 1000 C atoms)	9.6	9.7
M_n	4.27×10^4	2.73×10^4
M_w	9.65×10^4	1.21×10^5
M_w/M_n	2.3	4.4

[a] Reference 1.

DSC. DSC 2920 (TA Instruments) was operated at a heating rate of 10 °C/min. The sample mass of 2.5−2.8 mg was used. The instrument was calibrated with high-purity indium standards.

TEM. Specimens for TEM observations were stained in 0.5% RuO_4 aqueous solution at room temperature for 20 h and cut into ultrathin sections with a thickness of 70−80 nm with an ultrotome NOVA. TEM observations were conducted on a JEOL JEM-1200EX at an accelerating voltage of 120 kV.

Solid-State ^{13}C NMR. Solid-state ^{13}C NMR measurements were performed on a JEOL JNM-GSX 200 spectrometer operating under a static magnetic field of 4.7 T. Each sample

[⊗] Abstract published in *Advance ACS Abstracts,* November 1, 1997.

S0024-9297(97)00581-0 CCC: $14.00

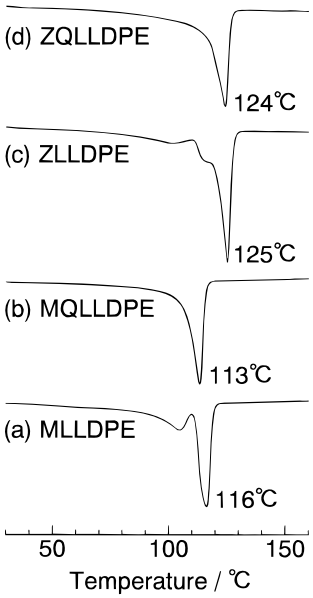

Figure 1. DSC curves for different LLDPE samples: (a) MLLDPE; (b) MQLLDPE; (c) ZLLDPE; (d) ZQLLDPE.

was packed into a 7 mm diameter zirconia rotor. ^{1}H and ^{13}C radio frequency fields $\gamma B_1/2\pi$ were 61.0−62.5 and 55.6−64.1 kHz, respectively. The contact time for the cross-polarization (CP) process was 1.0 ms throughout this work. The magic angle spinning (MAS) rate was set to 3 kHz to avoid the overlapping of spinning side bands on other resonance lines. ^{13}C chemical shifts were expressed as values relative to tetramethylsilane (Me_4Si) by using the CH_3 line at 17.36 ppm of hexamethylbenzene crystals as an external reference.

Results and Discussion

Figure 1 shows DSC curves for different LLDPE samples. The melting temperature of MLLDPE is determined to be 116 °C from the maximum endo heat flow. The lower peak at 105 °C is ascribed to partial melting of thinner crystallites shown in electron micrographs below. Such small crystallites are thought to be generated at the cooling process from the crystallization temperature of 110 °C to room temperature. The melting temperature of MLLDPE is higher than that of MQLLDPE, reflecting the difference in crystallization conditions. Melting temperatures of ZLLDPE and ZQLLDPE are higher than those of metallocene-catalyzed samples. This means that the lamellar thickness is larger in ZLLDPE and ZQLLDPE than in metallocene-catalyzed samples.[1]

A transmission electron micrograph of MLLDPE is shown in Figure 2a. The white rodlike regions are crystalline lamellae. Most of the crystalline lamellae have an almost equal thickness of 8.6 nm. Thinner crystallites are also found, which are thought to be crystallized during the cooling process as described above. A transmission electron micrograph of MQLLDPE is shown in Figure 2b. Crystalline lamellae are as thin as 7.1 nm, and spherullites seem to be not well-developed in accord with the previous report.[21] Electron micrographs of ZLLDPE and ZQLLDPE are shown in Figure 2c,d, respectively. The lamellae observed for these samples are significantly thicker compared with those of the corresponding metallocene-catalyzed samples.

The relation between lamellar thickness l and melting

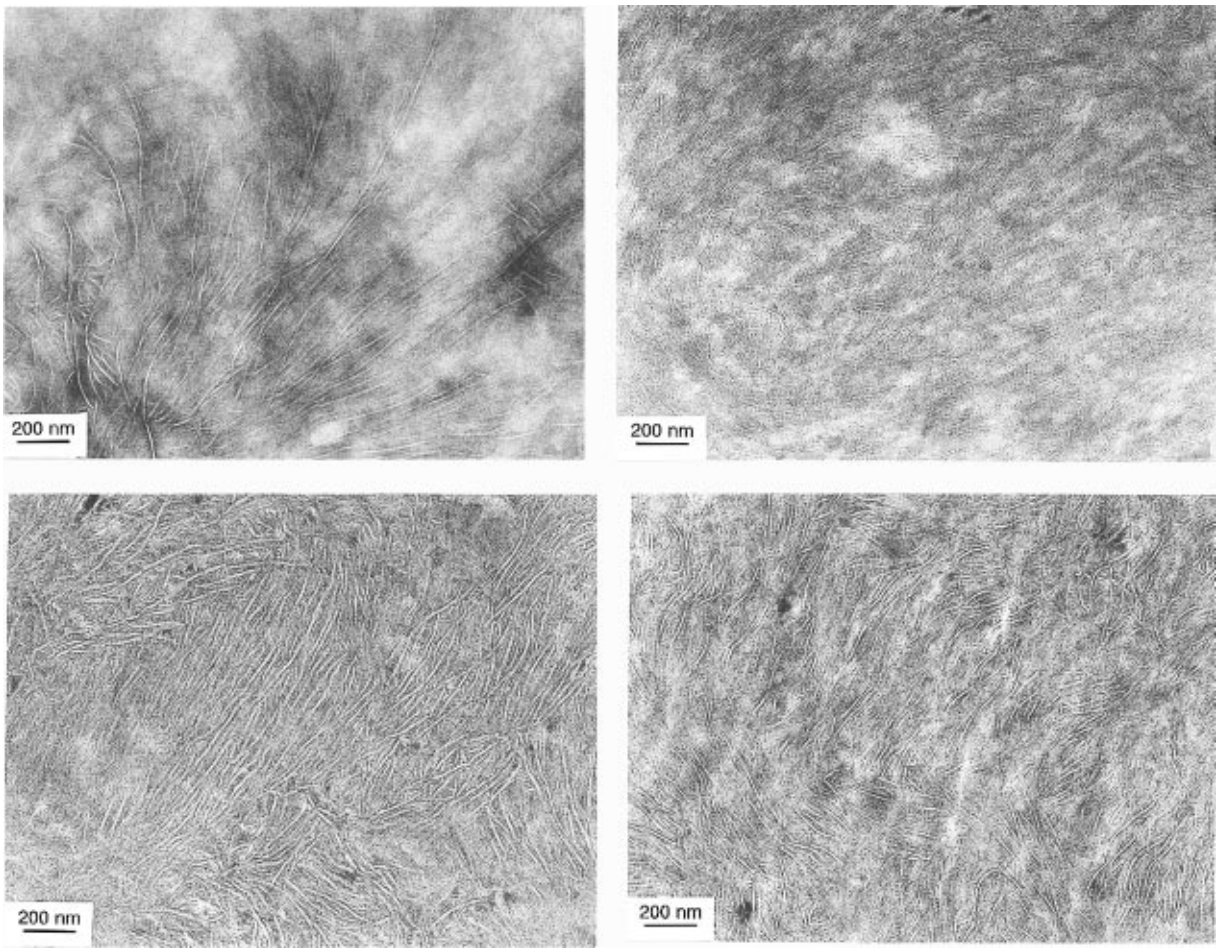

Figure 2. Transmission electron micrographs of different LLDPE samples stained by RuO_4: (a, top left) MLLDPE; (b, top right) MQLLDPE; (c, bottom left) ZLLDPE; (d, bottom right) ZQLLDPE.

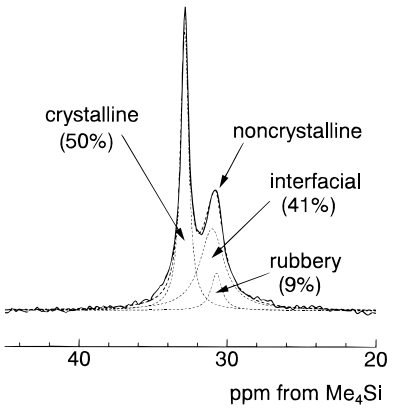

Figure 3. Fully relaxed DD/MAS ^{13}C NMR spectrum of MLLDPE.

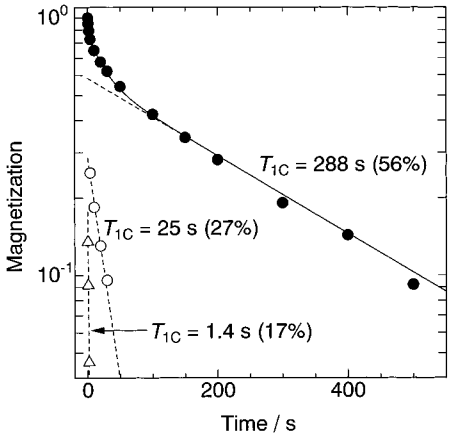

Figure 4. ^{13}C spin−lattice relaxation behavior of the crystalline component of MLLDPE obtained by the CPT1 pulse sequence.

temperature T_m is known as the following equation:[22,23]

$$T_m = T_m^0(1 - 2\sigma_e/\Delta h l) \quad (1)$$

where $T_m^0 = 415$ K, $\sigma_e = 93$ mJ m^{-2}, and $\Delta h = 300$ J cm^{-3} for polyethylene.[1] $T_m = 116$ °C for MLLDPE yields $l = 10.0$ nm, and $T_m = 113$ °C for MQLLDPE yields $l = 8.9$ nm. These values are not so different from the lamellar thicknesses obtained by TEM observations. Therefore, eq 1 is useful in these samples as a simpler way to estimate lamellar thicknesses.

A fully relaxed dipolar decoupling/MAS (DD/MAS) ^{13}C NMR spectrum of MLLDPE is shown as a thick solid line in Figure 3. The resonance line at 32.9 ppm is assigned to the orthorhombic crystalline component, whereas the line at 31 ppm is ascribed to the noncrystalline component.[7] The result of the line shape analysis shown by the dashed lines will be described below. For the purpose of obtaining more detailed information about the crystalline and noncrystalline components, ^{13}C spin−lattice relaxation time (T_{1C}) and ^{13}C spin−spin relaxation time (T_{2C}) are measured.

In Figure 4, the logarithmic peak intensities of the crystalline component, which were measured by the CPT1 pulse sequence,[24] are plotted against the decay time for the T_{1C} relaxation. The total decay curve appears not to be described in terms of a single exponential. Similarly to the cases of other polyethylene samples,[7,12,25] this decay curve can be resolved into three components with different T_{1C} values, as shown by the dashed lines in Figure 4. The composite curve (solid line) of the three components, obtained by the least-squares method, is in good accord with the observed data. It is therefore concluded that there also exist three components with $T_{1C} = 288$, 25, and 1.4 s in the crystalline component for MLLDPE.

Table 2. Physical Parameters Obtained for Different LLDPE Samples

samples	crystalline (orthorhombic)	noncrystalline	
		interfacial	rubbery
MLLDPE			
chemical shift/ppm	32.9	31.0	30.7
T_{1C}/s	288, 25, 1.4	0.41	0.41
T_{2C}/ms	*a*	0.060	4.3
mass fraction	0.50	0.41	0.09
lamellar thickness[b]/nm	8.6	3.2	*c*
MQLLDPE			
chemical shift/ppm	32.9	31.0	30.8
T_{1C}/s	121, 18, 1.9	0.44	0.44
T_{2C}/ms	*a*	0.057	4.0
mass fraction	0.45	0.42	0.13
lamellar thickness[b]/nm	7.1	3.2	*c*
ZLLDPE			
chemical shift/ppm	32.9	30.9	30.7
T_{1C}/s	488, 52, 2.0	0.38	0.38
T_{2C}/ms	*a*	0.071	6.3
mass fraction	0.57	0.32	0.11
lamellar thickness[b]/nm	12.4	3.3	*c*
ZQLLDPE			
chemical shift/ppm	32.9	31.0	30.7
T_{1C}/s	153, 27, 2.0	0.38	0.38
T_{2C}/ms	*a*	0.071	5.2
mass fraction	0.51	0.40	0.09
lamellar thickness[b]/nm	9.6	3.4	*c*

[a] Not measured. [b] Determined from electron micrographs. [c] The thickness cannot be determined because the rubbery component forms the continuous phase. See text.

The T_{1C} relaxation process for the noncrystalline component is measured by the saturation recovery pulse sequence modified for solid-state measurements[7,8] and well-analyzed in terms of a single component with $T_{1C} = 0.41$ s. The T_{1C} values thus obtained for all samples employed in this work are listed in Table 2. Each LLDPE sample consists of the crystalline, interfacial, and rubbery components like HDPE samples.[7,10,12,25,26] The longest T_{1C} value of MLLDPE is significantly shorter than the values for ZLLDPE as well as for bulk-crystallized HDPE.[7,27] Such differences are associated with the difference in lamellar thickness.[27]

The noncrystalline region seems to consist of only one component judging from the T_{1C} value which is associated with the molecular motion with the order of 10^8 Hz. In bulk-crystallized HDPE,[7,10,12] the noncrystalline region is further separated into the crystalline−amorphous interfacial and amorphous components by using the difference in T_{2C}'s measured under a condition without ^1H dipolar decoupling. Figure 5 is the ^{13}C spin−spin relaxation process of the noncrystalline component of MLLDPE measured by the ^{13}C spin-echo pulse sequence without ^1H dipolar decoupling.[7,8] Two components with different T_{2C} values are observed. In the analogy of the previous assignment,[7,10,12] the components with $T_{2C} = 60$ μs and 4.3 ms are assigned to the crystalline−amorphous interfacial and rubbery amorphous components, respectively. In fact, it was confirmed by ^1H spin diffusion measurements[10] that the interfacial component is really located between the crystalline and the rubbery amorphous components as schematically drawn in Figure 10. T_{2C} values obtained for the noncrystalline components are also listed in Table 2.

Using the difference in T_{2C}, the spectra of the interfacial and rubbery components were separately recorded by the same procedure as that described in the previous paper[7] in detail. These spectra can be well-described

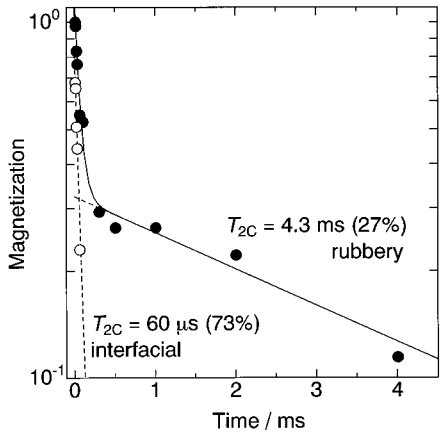

Figure 5. ^{13}C spin−spin relaxation behavior of the noncrystalline component of MLLDPE obtained by the ^{13}C spin-echo pulse sequence.

by single Lorentzian curves with given chemical shifts and line widths. Using these Lorentzian lines, a line shape analysis has been carried out for the fully relaxed DD/MAS ^{13}C NMR spectrum of MLLDPE. The result is shown in Figure 3, together with the integrated intensity fractions of the respective components. Although the crystalline line at 32.9 ppm comprises three components with different T_{1C}'s, the line is assumed to be a single Lorentzian. The composite curve of the three components is in good accord with the observed curve. The mass fractions for the crystalline, interfacial, and rubbery components are 0.50, 0.41, and 0.09, respectively. It is found that the mass fraction of the crystalline component agrees well with the degree of crystallinity (0.49) determined from the DSC curve shown in Figure 1. The lower crystallinity of this sample, compared with that of HDPE samples,[7] is due to the existence of butyl branches.

NMR relaxation parameters and the results of line shape analyses for MQLLDPE, ZLLDPE, and ZQLLDPE are also listed in Table 2. The lower crystallinity and shorter T_{1C} values of MQLLDPE compared with those of MLLDPE may be due to the quenching effect. The crystallinity of the sample prepared by the Ziegler−Natta process is higher than metallocene-catalyzed LLDPE crystallized under the same conditions. In comparison with T_{1C} values, crystalline components in ZLLDPE and ZQLLDPE have less mobility and relatively ordered structures than those of MLLDPE and MQLLDPE.

The partitioning of branches in the crystalline and noncrystalline regions in polyethylene is also an important problem.[28−32] It is reported that methyl branches are readily included in the crystalline region, while longer branches, such as butyl branches, are fully excluded out from this region under the equilibrium condition.[28−32] In order to clarify the distribution of butyl branches in the crystalline and noncrystalline regions, the following assumptions are made on the basis of the previous characterization.[29] First, this polyethylene sample is composed of three phases as described above. Second, ^{13}C signals obtained after ^{1}H−^{13}C CP for a given time are proportional to the polarization level (spin temperature) of the nearby protons. Third, during the CP period, branch protons in the respective regions will have polarization levels which are very close to those of their immediately neighboring main chain methylene protons, due to the efficient proton spin diffusion in the respective regions. The latter three assumptions were critically discussed by

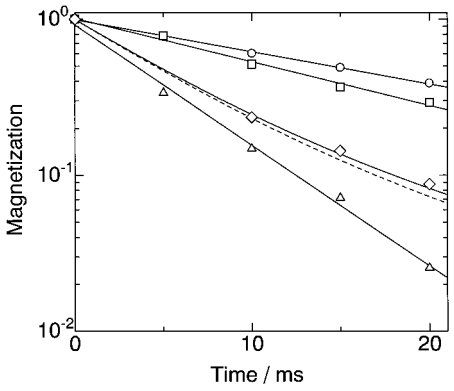

Figure 6. ^{1}H spin−lattice relaxation behavior in the rotating frame for MLLDPE: ○, crystalline component with $T_{1\rho H}$ = 21 ms; Δ, interfacial component with $T_{1\rho H}$ = 5.6 ms; □, rubbery component with $T_{1\rho H}$ = 16 ms; ◇, methyl carbons of butyl branches. The broken line is the linear combination of the decays of the interfacial and the rubbery components with $T_{1\rho H}$ = 5.6 and 16 ms with the fractions of 0.8 and 0.2, respectively.

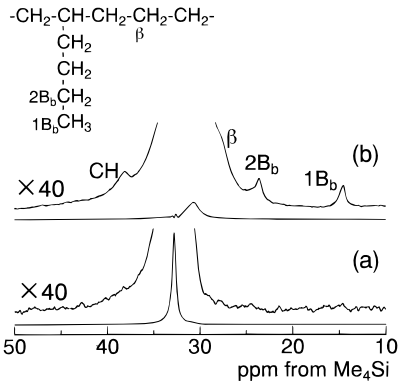

Figure 7. CP/MAS ^{13}C NMR spectra of the crystalline (a) and noncrystalline (b) components for MLLDPE. These spectra were obtained from the linear combination of CP/MAS ^{13}C NMR spectra measured for the $T_{1\rho H}$ decay times of 0, 10, and 15 ms by the combined pulse sequence of the ^{1}H spin-locking and CP procedures.

VanderHart and Pérez.[29] First we have measured ^{1}H spin−lattice relaxation times $T_{1\rho H}$'s in the rotating frame for the crystalline, interfacial, and rubbery components as well as for the CH_3 resonance line of the butyl branches by the combined pulse sequence of the ^{1}H spin locking and CP procedures. Figure 6 shows $T_{1\rho H}$ decays for the respective components and the CH_3 line, where the magnetizations of the respective components were obtained by the three component analysis shown in Figure 3. Each decay can be described as a single exponential except for the decay of the CH_3 line. This fact indicates that the ^{1}H spin diffusion among these three components is significantly low compared to the order of these $T_{1\rho H}$ values, in good accord with the previous results for the oriented polyethylene sample.[10] In the case of the CH_3 line, the observed decay is in good accord with the broken line that is the linear combination of the contributions from the interfacial and rubbery components considering their mass fractions, determined as shown in Figure 3. This fact will support such a possible assumption that butyl branches are equally distributed in the interfacial and rubbery regions. It should be noted here that the $T_{1\rho H}$ value of the interfacial component is much shorter than that of the rubbery component, suggesting the restricted molecular mobility of the former component compared to the latter component.

On the basis of these results of $T_{1\rho H}$ measurements, we have measured CP/MAS ^{13}C spectra for three $T_{1\rho H}$

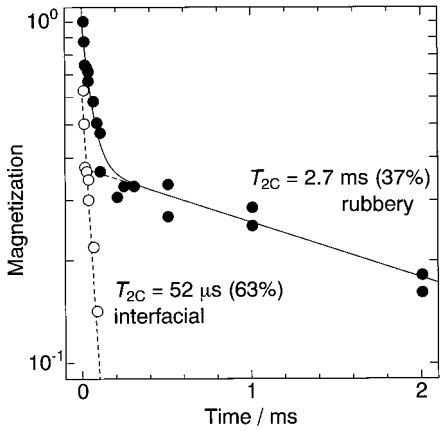

Figure 8. ^{13}C spin−spin relaxation behavior of the CH carbon at the branching point for MLLDPE obtained by the ^{13}C spin-echo pulse sequence.

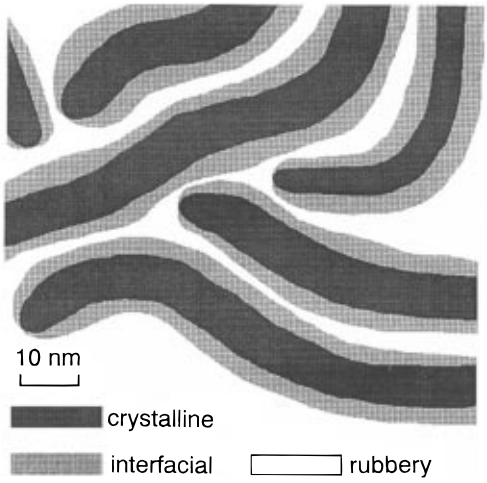

Lamellar thickness: crystalline 8.6 nm
interfacial 3.2 nm

Figure 9. Schematic morphological model for MLLDPE.

decay times of 0, 10, and 15 ms using the same pulse sequence as that for $T_{1\rho H}$ measurements in Figure 6. By the linear combination of these spectra, we can separately obtain the spectra of the crystalline and noncrystalline components as shown in Figure 7. The concentration of the butyl branches is found to be the noise level for the crystalline component, leading to the conclusion that all branches are excluded out from the crystalline region. This conclusion is in good agreement with the previous results.[28−32] In addition, further separation of the noncrystalline resonance line to the contributions from the interfacial and rubbery components was not carried out in this work, because the signal to noise ratios of the corresponding spectra were not high enough.

The partitioning of the butyl branches in the interfacial and rubbery regions has been investigated by analyzing the T_{2C} relaxation behavior measured for the CH carbon at the branching point by the ^{13}C spin-echo pulse sequence. Figure 8 shows the T_{2C} decay as closed circles for the CH carbon of MLLDPE. It is also found that for the branch carbon there exist two components with T_{2C} = 2.7 ms and 52 μs which are respectively assigned to the rubbery and interfacial components, in accord with the case for the main chain CH_2 carbons shown in Figure 5. The T_{2C} values for the branch CH carbons are somewhat shorter than that for the main chain carbons, indicating that the branching points are less mobile than the main chain methylene sequence. The mass fractions for the interfacial and rubbery components are 0.63 and 0.37, respectively. These values are quite close to the values 0.73 and 0.27 estimated for the main chain CH_2 carbons. It is, therefore, concluded that butyl branches are almost equally distributed in the interfacial and rubbery regions. For ZLLDPE, it is also concluded by the similar $T_{1\rho H}$ and T_{2C} analyses that the butyl branches are excluded from the crystalline region while butyl branches are almost equally partitioned in the interfacial and rubbery regions. There is no marked difference in the partitioning of branches in the crystalline and noncrystalline regions between MLLDPE and ZLLDPE.

Figure 9 shows the morphological model two-dimensionally drawn for MLLDPE on the basis of the results obtained by solid-state NMR analyses and TEM observations. Here, since the interfacial region is defined as a transitional region where the conformation is gradually randomized from the surface of the crystallites,[33] the thickness can be determined from the average thickness of crystalline lamellae and the volume fractions of the crystalline and interfacial components

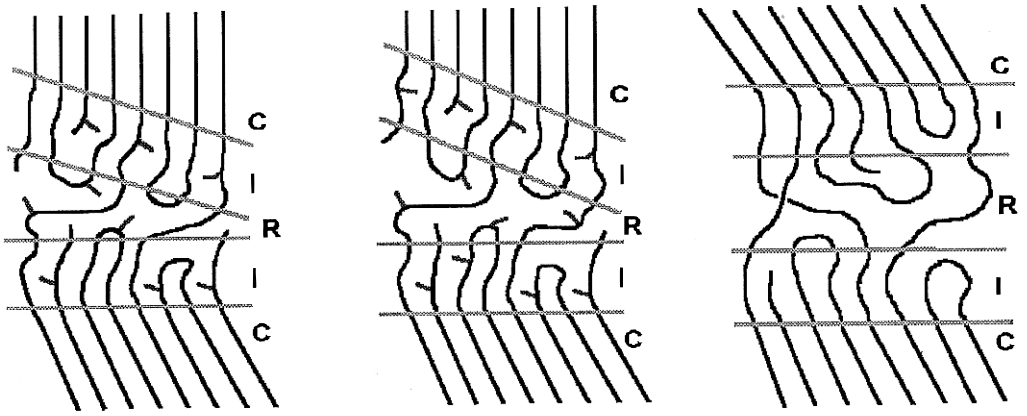

Figure 10. Molecular-level structure models for different polyethylene samples: C, crystalline; I, interfacial; R, rubbery.

without any information of the rubbery component. By assuming that the volume fractions are close to the mass fractions in this case, the thickness for the interfacial component is estimated to be about 3.2 nm. This value is in good accord with the value (3.4 nm) for the interfacial overlayer for bulk-crystallized HDPE[7] and the thickness (about 2.0 nm) of the crystalline−amorphous interphase that was deduced by Flory et. al.[33] from their theoretical calculation. The respective crystalline lamellae with the thickness of 8.6 nm are covered with the interfacial overlayer, and such lamellae are dispersed in somewhat disordered fashion in the continuous amorphous phase.

A molecular-level structure model for MLLDPE is shown in Figure 10 together with the models for ZLLDPE and HDPE. MLLDPE and ZLLDPE basically consist of the crystalline, interfacial, and amorphous regions in accord with the case of HDPE.[7,10,12] However, since butyl branches are excluded out from the crystalline region, the crystalline lamellae should be greatly decreased in thickness for MLLDPE and ZLLDPE compared with HDPE. These branches are almost equally distributed in the interfacial and amorphous regions in MLLDPE and ZLLDPE. The comonomer contents are almost the same for both LLDPE samples, as seen in Table 1, but crystalline lamellae for MLLDPE are significantly thinner than those for ZLLDPE. This fact may be due to the more random distribution of butyl branches in a chain for MLLDPE compared to the case of ZLLDPE. In addition, the comparison of T_{2C} values shown in Figure 10 suggests that the molecular mobility with the order of 10^5 Hz in the interfacial region is somewhat higher for ZLLDPE and MLLDPE than for HDPE, probably as a result of the plasticizing effect of branches.[34] It should be also noted that quenching has no significant effect on the basic crystalline−noncrystalline structure, including the interfacial structure, revealed for both LLDPE samples, although significant decreases in mass fraction and thickness are induced for the crystalline component by quenching.

Conclusion

The crystalline−noncrystalline structure for metallocene-catalyzed and Ziegler−Natta-catalyzed linear low-density polyethylene samples, isothermally crystallized or quenched from the melt, have been elucidated by high-resolution solid-state ^{13}C NMR spectroscopy, and the following conclusions have been obtained.

(1) ^{13}C spin−lattice relaxation time (T_{1C}) and ^{13}C spin−spin relaxation time (T_{2C}) analyses carried out at room temperature have confirmed the existence of three components, the crystalline, crystalline−amorphous interfacial, and rubbery amorphous components.

(2) The analyses of fully relaxed DD/MAS ^{13}C NMR spectra and transmission electron micrographs have revealed such a basic crystalline−noncrystalline structure that thin crystalline rods covered by the interfacial overlayers with a thickness of about 3 nm are dispersed in the continuous amorphous phase in a somewhat disordered fashion.

(3) Butyl branches are excluded out from the crystalline region and are almost equally distributed in the interfacial and amorphous regions.

(4) The difference between metallocene-catalyzed and Ziegler−Natta-catalyzed samples is mainly reflected on the differences in mass fraction and thickness for the crystalline component; these values are significantly smaller for the former than for the latter, probably due to the random distribution of branches for the former.

(5) Quenching effects appear mainly as decreases in crystallinity and thickness of crystalline lamellae, the basic crystalline−noncrystalline structure described above being almost unchanged.

Acknowledgment. We thank Mr. Yoshihiro Moteki, Ms. Yoshimi Shimizu, and Mr. Takashi Komazawa of Japan Polyolefins Co. Ltd. for taking transmission electron micrographs. We are also grateful to Professor Keisuke Kaji of Kyoto University for his kind support of our international cooperation and to the British Council for financial support of the exchange project. This work was partly supported by a Grant-in-Aid for Scientific Research (B) from the Ministry of Education, Japan (No. 08455453).

References and Notes

(1) Parker, J. A.; Bassett, D. C.; Olley, R. H.; Jaaskelainen, P. *Polymer* **1994**, *19*, 4140.
(2) Alamo, R. G.; Mandelkern, L. *Macromolecules* **1989**, *22*, 1273.
(3) Alamo, R. G.; Mandelkern, L. *Macromolecules* **1991**, *24*, 6480.
(4) Alamo, R. G.; Chan, E. M.; Mandelkern, L. *Macromolecules* **1992**, *25*, 6381.
(5) Sinn, H.; Kaminsky, W. *Adv. Organomet. Chem.* **1980**, *18*, 99.
(6) For example: (a) Schmidt-Rohr, K.; Spiess, H. W. *Multidimensional Solid-State NMR and Polymers*; Academic Press: London, 1994. (b) Blumich, B., Ed. *NMR Basic Principles and Progress. Solid-State NMR III Organic Matter*; Springler-Verlag: Berlin, 1994. (c) Tycho, R., Ed. *Nuclear Magnetic Resonance Probes of Molecular Dynamics*; Kluwer Academic Publishers: Dordrecht, The Netherlands, 1994.
(7) Kitamaru, R.; Horii, F.; Murayama, K. *Macromolecules* **1986**, *19*, 636, and related references of polyethylene cited therein.
(8) Hirai, A.; Horii, F.; Kitamaru, R.; Fatou, J. G.; Bello, A. *Macromolecules* **1990**, *23*, 2913.
(9) Saito, S.; Moteki, Y.; Nakagawa, M.; Horii, F.; Kitamaru, R. *Macromolecules* **1990**, *23*, 3257.
(10) Kimura, T.; Neki, K.; Tamura, N.; Horii, F.; Nakagawa, M.; Odani, H. *Polymer* **1992**, *33*, 4140.
(11) Tsuji, H.; Horii, F.; Nakagawa, M.; Ikada, Y.; Odani, H.; Kitamaru, R. *Macromolecules* **1992**, *25*, 4114.
(12) Kitamaru, R.; Horii, F.; Zhu, Q.; Bassett, D. C.; Olley, R. H. *Polymer* **1994**, *35*, 1171.
(13) Kaji, H.; Horii, F. *Macromolecules*, in press.
(14) Yamamoto, H.; Horii, F. *Macromolecules* **1993**, *26*, 1313.
(15) Yamamoto, H.; Horii, F. *Cellulose* **1994**, *1*, 57.
(16) Yamamoto, H.; Horii, F.; Hirai, A. *Cellulose* **1996**, *3*, 229.
(17) Horii, F.; Hu, S.; Ito, T.; Odani, H.; Matsuzawa, S.; Yamaura, K. *Polymer* **1992**, *33*, 2299.
(18) Hu, S.; Tsuji, M.; Horii, F. *Polymer* **1994**, *35*, 2516.
(19) Horii, F.; Masuda, K.; Kaji, H. *Macromolecules* **1997**, 30, 2519.
(20) Ishida, M.; Yoshinaga, K.; Horii, F. *Macromolecules* **1996**, 29, 8824.
(21) Mandelkern, L.; Glotin, M.; Benson, R. A. *Macromolecules* **1981**, *14*, 22.
(22) Flory, P. J. *J. Chem. Phys.* **1949**, *17*, 223.
(23) Flory, P. J. *J. Chem. Soc.* **1962**, *84*, 2857.
(24) Torchia, D. A. *J. Magn. Reson.* **1978**, *30*, 613.
(25) Shimizu, Y.; Harashina, Y.; Sugiura, Y.; Matsuo, M. *Macromolecules* **1995**, *28*, 6889.
(26) Horii, F.; Kitamaru, R. *J. Polym. Sci., Polym. Phys. Ed.* **1981**, *19*, 109.
(27) Axelson, D. E.; Mandelkern, L.; Popli, R.; Mathieu, P. *J. Polym. Sci., Polym. Phys. Ed.* **1983**, *21*, 2319.
(28) Alamo, R.; Domszy, R.; Mandelkern, L. *J. Phys. Chem.* **1984**, *88*, 6587.
(29) VanderHart, D. L.; Pérez, E.; *Macromolecules* **1986**, *19*, 1902.
(30) Pérez, E.; VanderHart, D. L. *J. Polym. Sci., Polym. Phys. Ed.* **1987**, *25*, 1637.
(31) Pérez, E.; VanderHart, D. L.; Crist, B., Jr.; Howard, P. R.; *Macromolecules* **1987**, *20*, 78.
(32) Bassett, D. C. *Developments in Crystalline Polymers 2*; Applied Science: London, 1988; pp 67−103.
(33) Flory, P. J.; Yoon, D. Y.; Dill, K. A. *Macromolecules* **1984**, *17*, 862.
(34) Nielsen, L. E. *Mechanical Properties of Polymers and Composites;* Marcel Dekker, Inc.: New York, 1975.

MA970581L